Reconstruction of forest litter horizons using ground-penetrating radar

Frédéric André, Mathieu Jonard
and Sébastien Lambot
Earth and Life Institute
Université catholique de Louvain
1348 Louvain-la-Neuve, Belgium
Email: frederic.andre@uclouvain.be,
mathieu.jonard@uclouvain.be, sebastien.lambot@uclouvain.be

François Jonard
Institute of Bio- and Geosciences
Forschungszentrum Jülich GmbH
52425 Jülich, Germany
Email: f.jonard@fz-juelich.de

***Abstract*—Forest litter constitutes a major component of forest ecosystems and its detailed characterization is necessary for thorough understanding and modeling of ecosystem functioning. Besides, the presence of litter is acknowledged to influence remote sensing radar data over forested areas and their proper processing requires accurate quantification of litter properties. In this work, ultra wideband (0.8-2.2 GHz) ground-penetrating radar (GPR) data were collected *in situ* for contrasted litter types to examine the ability of the technique to reconstruct litter constitutive properties. GPR data were processed resorting to full-wave inversion. Good agreement was generally observed between measured and estimated litter layer thicknesses. Yet, no significant correlation was found between both sets of values for recently fallen litter (OL layer) as a result of relatively large estimation and measurement errors compared with the limited variation range of this parameter. Furthermore, discrepancies between litter thickness estimates and measurements were also partly ascribed to weak dielectric contrasts both amongst litter layers and between litter and the organo-mineral A horizon. Reliable estimates of litter electromagnetic properties were also obtained from radar signal inversions. These results show promising potentialities of GPR for non-invasive characterization and mapping of forest litter.**

I. Introduction

Decomposing litter accumulated at the soil surface in forests play a major role in a series of ecological processes [1]–[5]. In other respects, the presence of forest litter is known to influence remote sensing radar data over forested areas and precise determination of litter radiative properties is necessary for proper processing of these data [6]–[8]. Forest litter thickness and composition may present large spatial variability under the combined influence of stand characteristics with climatic, biological and anthropogenic factors [9], [10]. Yet, the methods traditionally used for humus characterization are tedious and disturbing. In contrast, ground-penetrating radar (GPR) appears as being a particularly convenient tool for efficient and non-invasive characterization of litter layers. Besides, GPR would also allow for the investigation of the effect of litter on the radar signal. In this regard, André *et al.* [11] recently demonstrated the ability of GPR to retrieve the constitutive properties of artificially reconstructed litter layers through full-wave inversion of radar data. The present study was designed in the continuity of this work and aimed at investigating the potentialities of GPR to retrieve litter horizon properties in undisturbed natural conditions. This paper mainly focuses on the results relating to the retrieval of litter layer thicknesses from GPR. More complete outcomes of this study are presented in André *et al.* [12]

II. Material and methods

A. Experimental setup

The experiment was conducted within the "Bois de Lauzelle", located nearby the city of Louvain-la-Neuve in central Belgium. GPR data were collected together with reference measurements at 21 locations placed around every 5 m along a 100 m length transect through stands of various deciduous and coniferous tree species (Figure 1). The transect was especially defined so as to cross a wide range of litter characteristics in terms of thickness and composition. At each measurement location, GPR measurements were carried out at three different positions: a central measurement on the transect axis and two lateral measurements 2 m apart on each side along a line perpendicular to the transect axis. These pseudoreplicates aimed to capture the local spatial variability of litter properties around each measurement location. Furthermore, radar measurements were repeated twice at each position. Subsequently to radar measurements, litter was characterized at the central position of each measurement location by monolith sampling using a square 0.1 m^2 area metal frame and the litter layer thicknesses were measured to the nearest millimeter using a measuring tape. Two litter horizons were distinguished: the OL layer consisting of recently fallen litter with easily discernible plant organs and the OF layer corresponding to fragmented litter in partial decomposition without entire plant organs. Thickness measurements were performed in the middle of each side of the sampling square. Following these ground truth measurements, litter was removed over wider areas (c.a. 1.0 m $\times$ 1.0 m) centered on each sampling location. A second set of radar data was then collected for characterizing the properties of the organo-mineral A horizon, which was considered as the bottom layer of the litter profile (i.e., lower half-space of the electromagnetic model configuration).

B. Radar measurements and modeling

The GPR measurements were carried out using an ultra wideband stepped-frequency continuous-wave radar connected

978-1-4799-6495-6/15/$31.00

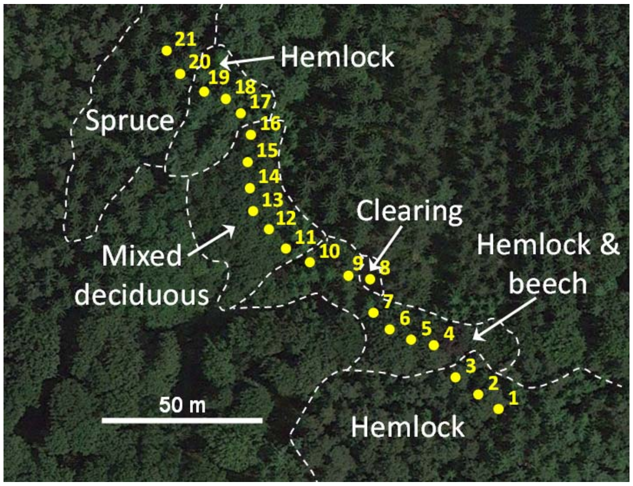

Fig. 1. Location of the measurement and sampling points. The dashed lines represent the limits of the crossed forest stands. (modified from Google Earth)

to a transmitting and receiving double-ridge horn antenna operating at around 30 cm above the medium. The antenna was connected to the reflection port of a vector network analyzer (VNA). The frequency-dependent complex ratio S_{11} between the returned and the emitted signals was measured sequentially at 234 evenly stepped frequencies from 0.8 to 2.2 GHz with a frequency step of 6 MHz. The antenna being located in the far-field region [13], the GPR data were processed using the far-field radar equation proposed by Lambot *et al.* [14], [15] formulated as follows in the frequency domain:

$$S_{11}(f) = \frac{b(f)}{a(f)} = R_0(f) + \frac{T_{\mathrm{S}}(f)G_{xx}^{\uparrow}(f)T_{\mathrm{i}}(f)}{1 - G_{xx}^{\uparrow}(f)R_{\mathrm{S}}(f)} \tag{1}$$

where $S_{11}(f)$ is the measured complex ratio between the backscattered $b(f)$ and the incident $a(f)$ fields at the VNA reference plane, $R_0(f)$ is the global reflection coefficient of the antenna in free space, $T_i(f)$ and $T_s(f)$ are the global transmission coefficients for fields incident from the VNA reference calibration plane onto the point source and for the field incident from the layered medium onto the field point, respectively, accounting for the gain and phase delay, and $R_s(f)$ is the global reflection coefficient for the field incident from the layered medium onto the field point accounting for the interactions between the antenna and the medium. $G_{xx}^{\uparrow}(f)$ is a Green's function representing the response of the air-subsurface system and is formulated as an exact solution of the 3-D Maxwell's equations for electromagnetic waves propagating in planar layered media. It is defined as the $x-$directed component of the reflected electric field for a unit-strength $x-$directed electric source. The antenna transfer functions $R_0(f)$, $T(f) = T_i(f)T_s(f)$ and $R_s(f)$ are determined from radar measurements over well characterized medium configurations for which the corresponding Green's functions can be readily computed. Then, after having been determined, these antenna transfer functions may be used to filter all antenna effects out of raw GPR data, thereby providing the observed Green's function $G_{xx}^{\uparrow meas}(f)$ which corresponds to the medium response only. Indeed, rearranging Equation (1), we have:

$$G_{xx}^{\uparrow meas}(f) = \frac{S_{11}(f) - R_0(f)}{S_{11}(f)R_s(f) + T_s(f)T_i(f) - R_0(f)R_s(f)} \tag{2}$$

A four-layer electromagnetic model was considered for the analysis of the GPR data acquired in the presence of litter, while a two-layer model was used for processing the data after litter removal. In both model versions, the upper and the lower layers correspond to the air layer between the antenna phase center and the litter surface and the A horizon defined as the lower half-space, respectively. The two intermediate layers of the four-layer represent the OL and OF litter horizons, respectively. Based on the results of André *et al.* [11], frequency dependence of litter effective electrical conductivity was considered to account for both scattering and dielectric losses occurring within litter horizons using the following linear equation:

$$\sigma(f) = \sigma_{0.8GHz} + a(f - 0.8 \times 10^9) \tag{3}$$

where $\sigma_{0.8GHz}$ is the reference electrical conductivity at 0.8 GHz and a is the linear variation rate of $\sigma(f)$.

Besides, as an alternative to the preceding approach accounting for both scattering and relaxation phenomena through frequency dependence of litter effective electrical conductivity, GPR data have also been processed by combining a roughness model with the radar model, as proposed by Jonard *et al.* [16]. This latter approach would potentially allow for a more physical description of electromagnetic wave scattering occurring due to litter surface roughness. Furthermore, it would also permit to quantify scattering apart from dielectric losses. The roughness model applied in this study is derived from the Kirchhoff scattering theory and describes the scattering losses in the specular direction due to the reflection on a rough interface [17]. In this model, the global surface reflection coefficient is multiplied by a scattering loss factor (ρ), which notably depends on the standard deviation of the surface height (s_r). Jonard *et al.* [16] successfully applied this approach to soil and we refer to this work for further details on the integration of the roughness model into the GPR model.

C. Model inversion

In a first step, the relative dielectric permittivity of the A horizon was determined from the radar data acquired after litter removal by performing GPR signal inversion in the time domain by focusing on a time window containing the surface reflection only, as proposed by Lambot *et al.* [18]. In a second step, the relative dielectric permittivity of the lower half-space of the four-layer electromagnetic model was set to the value found in the first step for $\varepsilon_{r,A}$ at the corresponding measurement location. Litter constitutive properties (i.e., layer thicknesses (h_{OL} and h_{OF}), layer relative dielectric permittivities ($\varepsilon_{r,OL}$ and $\varepsilon_{r,OF}$) and frequency dependence parameters for litter effective electrical conductivity ($\sigma_{0.8GHz,OL}$, $\sigma_{0.8GHz,OF}$, a_{OL} and a_{OF})) were then retrieved through full-wave inversion of the radar signal. We refer to André *et al.* [11] for more details on the processing of the radar data.

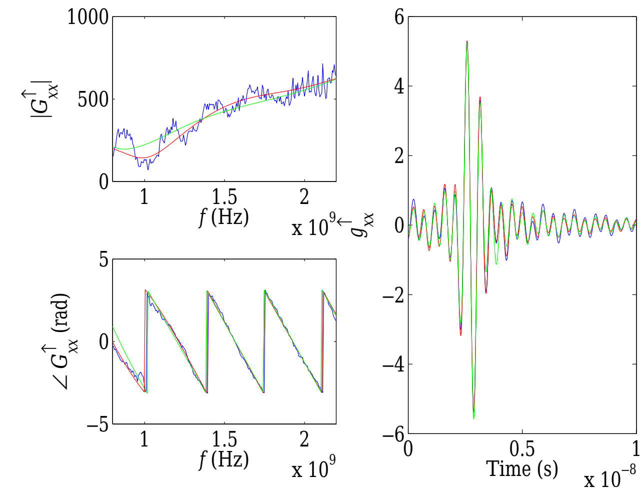

Fig. 2. Measured (blue curves) and modeled Green's functions in the frequency and the time domains for litter in the Spruce stand (location ♯21 along the measurement transect). The green and red curves represent the modeled Green's functions with the model versions with and without consideration of the roughness model, respectively.

III. Results and Discussion

As illustrated in Figure 2 for a measurement above litter in the Spruce stand, good agreement was generally observed between modeled and measured radar signals. In particular, the phase in the frequency domain and, consequently, the propagation time in the time domain were in most cases properly described by the model, while some discrepancies were sometimes found between the amplitude of the measured and modeled signals. Similar observations were reported for the controlled experiment [11]. Finally, some differences were also sometimes observed between Green's functions modeled with and without consideration of the roughness model, as it is notably the case for the data presented in Figure 2.

Figure 3(a), (b) and (c) present model inversion estimates for, respectively, OL and OF litter layer thicknesses (h_{OL} and h_{OF}) and for total litter thickness (h_{OL} + h_{OF}) as a function of the corresponding measured values, without considering the roughness model. Rather good correspondence is generally found between estimated and measured values for h_{OF} and h_{OL} + h_{OF}, while much weaker agreement is observed for h_{OL}. Considering all measurement locations, correlation coefficients between both sets of values amount to 0.36, 0.51 and 0.64 for OL, OF and OL+OF litter thicknesses, respectively, but drop to -0.01, 0.37 and 0.44 when discarding the two points presenting extreme high measured values for h_{OL} and h_{OL} + h_{OF} in the mixed Hemlock and beech stand. The lack of correlation for h_{OL} would at least partly arise from the much narrower range of values in effect for this parameter compared with that for h_{OF} and h_{OL} + h_{OF}. Indeed, as shown by the vertical and horizontal error bars representing 95% confidence intervals to average estimated and measured values, respectively, the range of values for h_{OL} is close to the order of magnitude of its estimation and measurement errors. Regarding h_{OF} (Fig. 3(b)), the main discrepancies between estimates and measurements are overestimations of the parameter that occur for its lowest measured values, corresponding to deciduous stand situations. These discrepancies attenuate for total litter thickness (Fig. 3(c)), revealing that the overestimations observed for h_{OF} were partly associated with underestimations of h_{OL} at the corresponding measurement locations. This would indicate inaccurate delineation of these two horizons from GPR signal inversion in these cases. Yet, some significant overestimations are still observed at some deciduous locations for total litter thickness (Fig. 3(c)), which would then presumably arise from a weak contrast between litter layers and the A horizon at these locations. This statement is corroborated by the quite close values observed for the estimated relative dielectric permittivity of the different layers in these cases, averaging to 3.0, 4.7 and 5.1 for the OL, the OF and the A horizons, respectively. On the other hand, it is worth noting that such observations could also partly result from difficulties in the visual delimitation of these layers as well as from the local spatial variability of their thicknesses at the sampling scale, leading to inaccuracy of the ground truth measurements. All situations together, estimated relative dielectric permittivities averaged to 3.1, 5.9 and 7.4 for the OL, the OF and the A horizons, respectively, which are in agreement with findings of André *et al.* [11].

Regarding results with consideration of the roughness model, relatively good agreement is also generally observed between estimated and measured litter layer thickness, as illustrated in Figure 3(d) for h_{OL} + h_{OF}. Estimates of litter relative dielectric permittivity are quite similar to that found without the roughness model, with average values of 4.2 and 7.1 for the OL and the OF layers, respectively. However, these values show larger variability than with the preceding approach, both amongst repetitions for a given measurement location and amongst locations (data not shown). Besides, the average value obtained for parameter s_r amounts to 0.013 m, which appears as plausible from visual examination of the spatial microvariability of the litter surface level. Yet, this constitutes preliminary results and further work is in progress in this direction to confirm and refine these observations with the aim of improving the modeling of the backscattering from the forest floor and quantify scattering apart from the dielectric losses occurring within litter.

IV. Conclusion

In continuation of a previous controlled experiment [11], this study evaluated the potentialities of GPR for *in situ* quantitative characterization of forest floor organic horizons by providing estimates of litter layer thicknesses and constitutive properties. Though the agreement between estimated and reference layer thickness values was somewhat lower than that observed in controlled conditions, the results generally showed the ability of the technique to retrieve litter layer thicknesses with reasonable accuracy, particularly for the OF and the total litter horizons. Reliable estimates of litter electromagnetic properties were also obtained. These results show promising potentialities of GPR for non-invasive characterization and mapping of forest litter.

Acknowledgment

This research was supported by the Fonds National de la Recherche Scientifique (FNRS, Belgium), the Université catholique de Louvain (UCL, Belgium) and Forschungszentrum Jülich GmbH (FZJ, Germany).

References

[1] F. Kostel-Hughes, T. P. Young, and J. D. Wehr, “Effects of leaf litter depth on the emergence and seedling growth of deciduous forest tree species in relation to seed size,” *Journal of the Torrey Botanical Society*, vol. 132, no. 1, pp. 50–61, 2005.

[2] M. Jonard, F. André, F. Jonard, N. Mouton, P. Proces, and Q. Ponette, “Soil carbon dioxide efflux in pure and mixed stands of oak and beech,” *Annals of Forest Science*, vol. 64, no. 2, pp. 141–150, 2007.

[3] M. Jonard, L. Augusto, C. Morel, D. L. Achat, and E. Saur, “Forest floor contribution to phosphorus nutrition: experimental data,” *Annals of Forest Science*, vol. 66, no. 5, p. 510, 2009.

[4] J. F. Ponge, “Plant-soil feedbacks mediated by humus forms: A review,” *Soil Biology & Biochemistry*, vol. 57, pp. 1048–1060, 2013.

[5] A. Rasoulzadeh and M. Homapoor Ghoorabjiri, “Comparing hydraulic properties of different forest floors,” *Hydrological Processes*, vol. 28, no. 19, pp. 5122–5130, 2014.

[6] J. P. Grant, A. A. Van de Griend, M. Schwank, and J. P. Wigneron, “Observations and modeling of a pine forest floor at L-band,” *IEEE Transactions on Geoscience and Remote Sensing*, vol. 47, no. 7, pp. 2024–2034, 2009.

[7] M. Kurum, P. E. O’Neill, R. H. Lang, M. H. Cosh, A. T. Joseph, and T. J. Jackson, “Impact of conifer forest litter on microwave emission at L-band,” *IEEE Transactions on Geoscience and Remote Sensing*, vol. 50, no. 4, pp. 1071–1084, 2012.

[8] R. Rahmoune, P. Ferrazzoli, Y. K. Singh, Y. H. Kerr, P. Richaume, and A. Al Bitar, “SMOS retrieval results over forests: Comparisons with independent measurements,” *IEEE Journal of Selected Topics in Applied Earth Observations and Remote Sensing*, vol. 7, no. 9, pp. 3858–3866, 2014.

[9] M. Jonard, F. André, and Q. Ponette, “Modeling leaf dispersal in mixed hardwood forests using a ballistic approach,” *Ecology*, vol. 87, no. 9, pp. 2306–2318, 2006.

[10] ——, “Tree species mediated effects on leaf litter dynamics in pure and mixed stands of oak and beech,” *Canadian Journal of Forest Research-Revue Canadienne De Recherche Forestière*, vol. 38, no. 3, pp. 528–538, 2008.

[11] F. André, M. Jonard, and S. Lambot, “Non-invasive forest litter characterization using full-wave inversion of microwave radar data,” *IEEE Transactions on Geoscience and Remote Sensing*, vol. 53, no. 2, pp. 828–840, 2015.

[12] F. André, F. Jonard, M. Jonard, and S. Lambot, “*In situ* characterization of forest litter using ground-penetrating radar,” submitted.

[13] A. Tran, F. André, C. Craeye, and S. Lambot, “Near-field or far-field full-wave ground penetrating radar modeling as a function of the antenna height above a planar layered medium,” *Progress in Electromagnetics Research*, vol. 141, pp. 415–430, 2013.

[14] S. Lambot, E. C. Slob, I. van den Bosch, B. Stockbroeckx, and M. Vanclooster, “Modeling of ground-penetrating radar for accurate characterization of subsurface electric properties,” *IEEE Transactions on Geoscience and Remote Sensing*, vol. 42, no. 11, pp. 2555–2568, 2004.

[15] S. Lambot and F. André, “Full-wave modeling of near-field radar data for planar layered media reconstruction,” *IEEE Transactions on Geoscience and Remote Sensing*, vol. 52, no. 5, pp. 2295–2303, 2014.

[16] F. Jonard, L. Weihermüller, H. Vereecken, and S. Lambot, “Accounting for soil surface roughness in the inversion of ultrawideband off-ground GPR signal for soil moisture retrieval,” *Geophysics*, vol. 77, no. 1, pp. H1–H7, 2012.

[17] W. S. Ament, “Toward a theory of reflection by a rough surface,” *Proceedings of the IRE*, vol. 41, no. 1, pp. 142–146, 1953.

[18] S. Lambot, L. Weihermüller, J. A. Huisman, H. Vereecken, M. Vanclooster, and E. C. Slob, “Analysis of air-launched ground-penetrating radar techniques to measure the soil surface water content,” *Water Resources Research*, vol. 42, no. 11, p. W11403, 2006.

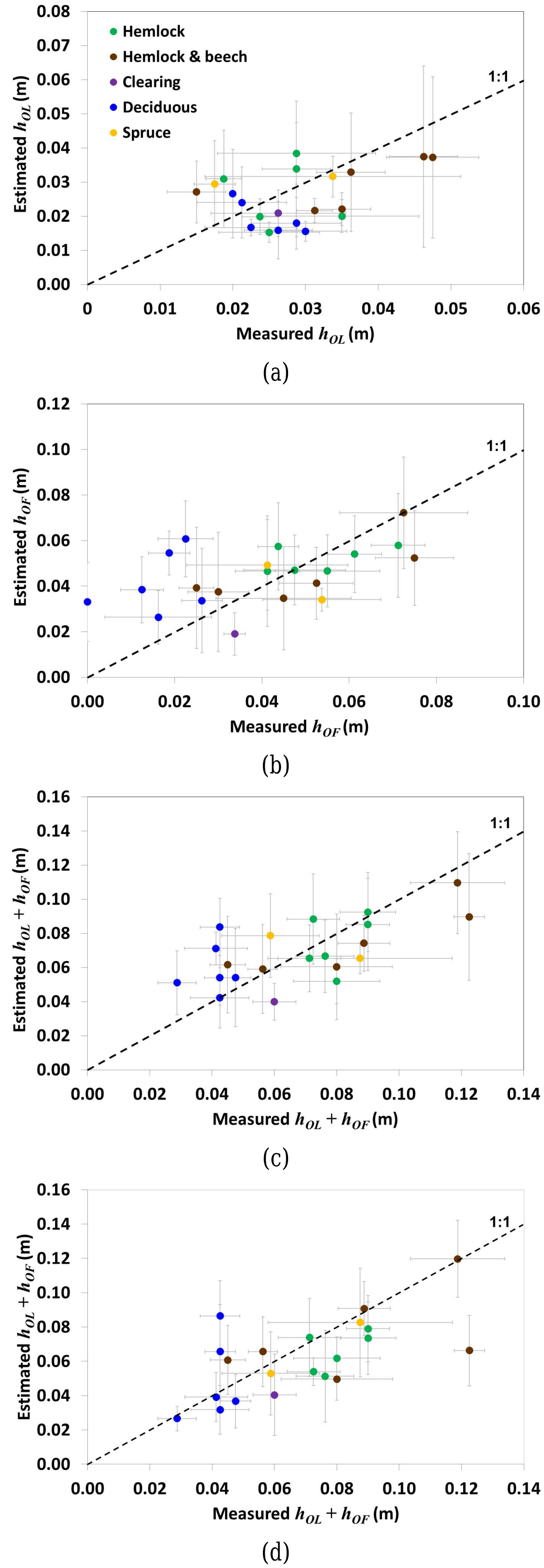

Fig. 3. Comparison of model inversion estimates for (a) OL litter layer thickness h_{OL}, for (b) OF litter layer thickness h_{OF} and for (c) total litter thickness $h_{OL} + h_{OF}$ with corresponding measured values without considering the roughness model, and for (d) total litter thickness when considering the roughness model. Results are presented specifying the stand composition at each measurement location. Vertical and horizontal error bars represent 95% confidence intervals for the six estimated values and for the four measured values at each location, respectively. The dashed line is the 1:1 line.